ACS APPLIED MATERIALS & INTERFACES

LETTER

www.acsami.org

Cationic Phenylene Ethynylene Polymers and Oligomers Exhibit Efficient Antiviral Activity

Ying Wang,[†,‡] Taylor D. Canady,[†] Zhijun Zhou,[†] Yanli Tang,[†] Dominique N. Price,[§] David G. Bear,[‡] Eva Y. Chi,[*,†] Kirk S. Schanze,[∥] and David G. Whitten[*,†]

[†] Department of Chemical and Nuclear Engineering, Center for Biomedical Engineering, [‡] Department of Chemistry and Chemical Biology and Department of Cell Biology and Physiology, [§]College of pharmacy, University of New Mexico, Albuquerque, New Mexico 87131-1341, United States [∥] Department of Chemistry, University of Florida, Gainesville, Florida 32611-7200, United States

ABSTRACT: The antiviral activities of poly(phenylene ethynylene) (PPE)-based cationic conjugated polyelectrolytes (CPE) and oligo-phenylene ethynylenes (OPE) were investigated using two model viruses, the T4 and MS2 bacteriophages. Under UV/visible light irradiation, significant antiviral activity was observed for all of the CPEs and OPEs; without irradiation, most of these compounds exhibited high inactivation activity against the MS2 phage and moderate inactivation ability against the T4 phage. Transmission electron microscopy (TEM) and SDS polyacrylamide gel electrophoresis (SDS-PAGE) reveal that the CPEs and OPEs exert their antiviral activity by partial disassembly of the phage particle structure in the dark and photochemical damage of the phage capsid protein under UV/visible light irradiation.

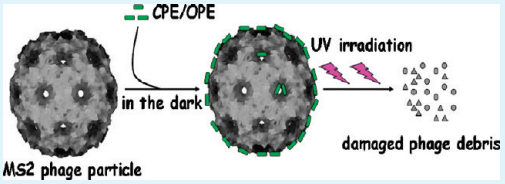

KEYWORDS: antiviral, cationic conjugated polyelectrolytes, cationic oligo-phenylene ethynylenes, T4 phage, MS2 phage, photoinduced antimicrobial activity

INTRODUCTION

Conjugated polymeric materials, such as poly(*para*-phenylene ethynylene) (PPE), poly(*para*-phenylene vinylene) (PPV), and poly(diacetylene) (PDA), exhibit unique size- and structure-dependent chemical and photophysical properties[1] and have various applications in electrically conducting materials, bio/chemical sensors, and supramolecular assemblies.[2] Recent work has shown that some cationic PPE-based polymers and oligomers display significant photoinducible antimicrobial activity in both Gram-positive and Gram-negative bacteria.[3] The direct contact between these antimicrobial compounds and microorganisms followed by the generation of corrosive reactive oxygen species (ROS) after exposure to UV−visible light appears to account for the high bactericidal activity of these cationic PPE-based compounds.[3a]

In addition to health threats caused by bacterial infections, many serious diseases are caused by viruses. The most notable example is human immunodeficiency virus induced acquired immune deficiency syndrome (HIV-AIDS), which has infected an estimated 33.3 million people.[4] Current interferon-based treatments for virus-caused diseases and current wastewater treatments against viral contamination are inadequate.[5] The development of new antiviral agents is a critical worldwide healthcare need. Given our increased understanding of the mechanism of dark and light-induced inactivation of bacteria by the PPE polymers and oligomers, we suspected that these materials might also be effective against viruses. Here, we investigate the antiviral activities of a series of CPEs and OPEs against two model viruses, the MS2 and T4 bacteriophages. The structures and compositions of these bacteriophages have been extensively investigated.[6] Bacteriophage MS2 is a nonenveloped, ∼27 nm RNA virus with a small single-stranded RNA genome of ∼3600 nucleotides. Its structure is very similar to some members of the picornavirus family, which are important human and animal viral pathogens.[7] Bacteriophage T4 is a relative large, nonenveloped 170 kbp double-stranded DNA virus with a 120 nm by 86 nm head and a 100 nm tail. These two bacteriophages are commonly used as model systems for environmental pollution and virus detection studies.[8]

The isoelectric points of the MS2 and T4 phage particles are 3.9 and 4−5, respectively,[9] which render them slightly negatively charged in neutral buffers. Thus, our cationic CPEs and OPEs are expected to readily associate with the phage particles and possibly attenuate their recognition and binding to host cells. Previously, we proposed that after exposure to UV−visible light, the CPEs and OPEs can generate singlet oxygen species followed by the formation of more corrosive reactive oxygen intermediates.[3a] This property of the CPEs and OPEs is due to the conjugated π bonding system in the backbone of the compounds, which allows for efficient intersystem crossing to a triplet state that sensitizes the formation of singlet oxygen $^1O_2$. $^1O_2$ and the subsequent ROS intermediates are known to be highly damaging to biomolecules, including proteins, RNA, and DNA.[10] In addition, the association of CPEs and OPEs with biological structures, in the absence of any irradiation, has been shown to disrupt noncovalent biomolecular assemblies, including the lipid

Received: May 9, 2011
Accepted: June 13, 2011
Published: June 13, 2011

ACS Publications © 2011 American Chemical Society

Scheme 1. Structures of the Antimicrobial Compounds Used in This Study[a]

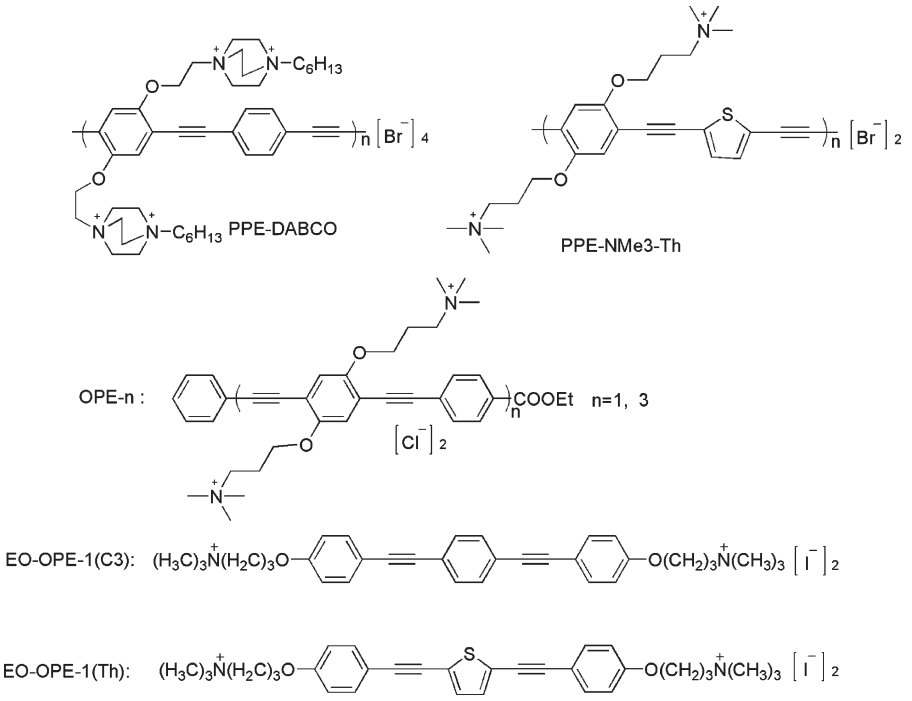

[a] *n* denotes the number of repeat units.

membrane[11] and folded protein structures. The major components of viruses are proteins, RNA, or DNA. Moreover, the virus capsid, which encloses the genetic material of the virus, is made of noncovalently assembled proteins.

In the current study, we evaluate the antiviral activities of a number of CPE and OPE compounds against two model viruses in the presence and absence of UV or short wavelength visible light using biological (infectivity) and morphological structural (TEM) assays. SDS-PAGE provides additional insights into the mechanism of the light-induced inactivation mechanism of CPEs and OPEs.

EXPERIMENTAL METHODS

Materials. The novel antimicrobial materials (Scheme 1) were synthesized as previously reported.[3c,12] Luria broth (LB) and agar were purchased from BD Biosciences (Franklin Lakes, NJ). All other chemicals were purchased from Sigma-Aldrich (St. Louis, MO) or Bio-Rad (Hercules, CA). Bacteriophages MS2 and T4 were obtained from the American Type Culture Collection (ATCC, Manassas, VA) along with their host bacteria, *E. coli* ATCC 15597 and *E. coli* ATCC 11303. Ultrapure water was used throughout the study (Milli-Q, 18.2 MΩ cm^{-1} resistivity).

Bacteriophage Preparation and Titer. *E. coli* cells were grown in LB. The fresh *E. coli* culture was inoculated from an overnight culture, followed by approximately three hours of incubation at 37 °C to the exponential growth phase ($O.D._{600} \sim 0.5$). *E. coli* cells were then collected by centrifugation and washed twice with *E. coli* minimal medium (glucose 28 mM, Na_2HPO_4 42 mM, KH_2PO_4 22 mM, NH_4Cl 18.7 mM, NaCl 8.5 mM, $MgSO_4$ 1 mM, and $CaCl_2$ 0.09 mM at pH 7.2) . The cell pellet was then resuspended in the minimal medium. An aliquot of phage stock solution was added to the corresponding bacterial host suspension and the phage-bacteria mixture was incubated for 15 min at 37 °C. The mixture was then transferred into fresh *E. coli* minimal medium and incubated overnight for viral replication and cell lysis. The phage solution was then centrifuged at 3500 rpm for 30 min, and the supernatant was filtered using 0.22 μm filters to remove unlysed bacteria and bacterial debris. The phage titer was determined by plaque forming units (PFU). Briefly, *E. coli* cells in the exponential growth phase (ATCC 15597 and 11303 for MS2 and T4 bacteriophage, respectively) were incubated with the various dilutions of the phage solution for 15 min at 37 °C and then transferred into molten soft LB agar with gentle mixing. The soft agar mixture was then poured onto presolidified LB plates. After incubation for 6−8 h, the numbers of PFU were counted and phage solutions were diluted to $10^6 \sim 10^7$ PFU/mL with the minimal medium for further use.

Phage Inactivation. CPE and OPE solutions (10 μg/mL) were incubated with virus solutions in the dark or under UV light for 1 h. The UV light irradiation experiments were carried out in a photoreactor (LZC-ORG, Luzchem Research Inc., Ottawa, Canada). Two illumination sources were employed due to the different light-absorbing properties of the CPEs and OPEs. UVA (centered at ∼350 nm) and LZC-420 (centered at ∼420 nm) were used to irradiate OPEs and CPEs, respectively. The viral inactivation ability of a CPE or an OPE was determined by phage titer as described in the previous section and calculated as log (N_o/N), where N is the PFU of the phage solution after exposure to a CPE or an OPE and N_o is the PFU of a control (without CPEs, OPEs, or UV irradiation). Log (N_o/N) reduced by the different treatments compared to control are reported. The reported values were averages of duplicate measurements.

Transmission Electron Microscopy. High concentrations of the viruses ($\sim 10^{11}$ PFU/mL for T4 and $\sim 10^{12}$ PFU/mL for MS2) and CPE or OPE (50 μg/mL) were used for TEM imaging (Hitachi H7500, Tokyo, Japan). The same phage inactivation

protocol was used as described in the previous section. Samples (5 μL) were applied to freshly cleaned carbon-coated copper grids, washed with pure water, and negatively stained with 2% uranyl acetate for 2 min. The grids were then dried in air and imaged at 70−100K fold magnification with 200 μm condenser aperture and 20 μm objective aperture.

SDS-PAGE. SDS-PAGE method was used to characterize MS2 phage capsid protein cleavage.[13] One liter of MS2 phage was prepared as described above and purified according to a modified protocol.[6a,14] Briefly, the purification of MS2 phage particle was performed by separating unlysed *E. coli* cells and cell debris by centrifugation followed by poly(ethylene glycol)-8000 (PEG-8000)/NaCl selective precipitation. After an overnight incubation at 4 °C, the fine precipitates were collected by centrifugation at 18000 rcf for 1 h at 4 °C. The pellet was collected and resuspended in TNM buffer (10 mM Tris, 100 mM NaCl and 0.1 mM $MgCl_2$ at pH 7.4). The phage suspension was passed through a 0.22 μm filter, and the filtrate was concentrated by an Amicon centrifuge filter with a molecular weight cutoff of 30000 (Millipore, Billerica, MA). Further purification of the phage particles was accomplished by Sepharose CL-4B (Sigma) column to remove residual PEG-8000, DNA, and RNA from the host cells. Then, the purified phage solution was incubated with EO-OPE-1(Th) under UV light or in the dark for 1 h. Then 20 μL of the inactivated phage sample was mixed with 10 μL of 3× standard SDS-PAGE sample loading buffer and heated in boiling water for 2 min. The denatured virus samples were loaded directly onto the gels. Electrophoresis was performed at 30 mA for approximately 1 h, after which the gel was stained with either silver (Silver Stain Plus Kit, Bio-Rad) or Coomassie brilliant blue R.

RESULTS AND DISCUSSION

The phage titer assay was carried out by a serial dilution of phage-CPE/OPE mixture and incubating each diluted sample with the corresponding *E. coli* host cells within molten soft LB agar. Since our previous work demonstrated that the CPEs/OPEs can efficiently inactivate *E. coli* cells,[3b,c,15] which may interfere with the plaque assay, it is necessary to study the effect of residual CPEs/OPEs on the *E. coli* host cells. For the control experiment without phage and CPEs/OPEs, *E. coli* forms a confluent cell sheet on the soft agar after 6 h of incubation at 37 °C. Under the current experimental conditions, 0.33 μg/mL was the maximum concentration of residual CPEs/OPEs in the soft agar (100 μL of inactivated phage sample by 10 μg/mL CPEs/OPEs was mixed with 3 mL of melted soft agar), which did not cause any obvious defects in the bacterial cell sheet.

CPEs and OPEs Exhibit Efficient Phage Inactivation Ability. Figure 1 summarizes T4 and MS2 phage inactivation induced by different CPE and OPE compounds in the dark (black bars) or with UV/visible irradiation (blue bars). The effect of irradiation alone (red bars) on phage inactivation was also determined. Even in the absence of UV or visible light, PPE-DABCO and EO-OPE-1(Th) exhibit significant antiviral activities against the T4 phage, reducing the number of PFU by 6 and 3 orders of magnitudes, respectively. In comparison, PPE-Th, OPE-1, and EO-OPE-1(C3) are less active in the dark, albeit inducing ca. 1 order of magnitude of inactivation. No dark inactivation activity is observed for OPE-3 against the T4 phage. UV irradiation enhanced the inactivation of the T4 phage induced by all CPEs and OPEs. For example, UV light enhanced PPE-Th and EO-OPE-1(C3)-induced inactivation

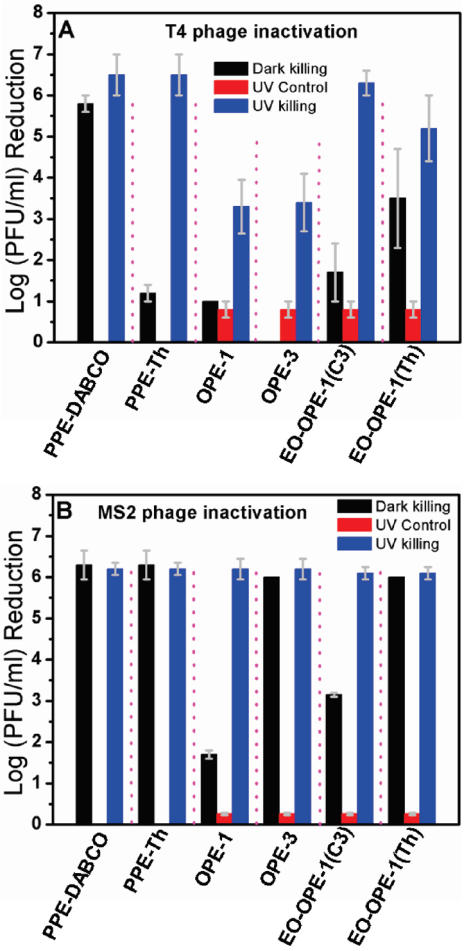

Figure 1. Inactivation of the T4 (A) and MS2 (B) bacterialphages by CPEs or OPEs in the dark (black bars) or with UV-light irradiation (blue bars). UV control samples (red bars) were those exposed to irradiation alone. The detection limit for the assay is 6−7 logs of PFU/mL.

by about 5 and 3 orders of magnitude compared to inactivation by the compounds in the dark. Whereas OPE-3 was ineffective in the dark, a 3 order of magnitude decrease in PFU was observed with UV irradiation.

Compared with the inactivation of T4 phage, all CPEs and OPEs tested were more efficient at inactivating the MS2 phage in the dark (Figure 1B). All compounds, except OPE-1 and EO-OPE-1(C3), induced more than 6-log inactivation against MS2 phage in the dark. With UV irradiation, OPE-1 and EO-OPE-1(C3) became very efficient at inactivating the MS2 phage.

Of the compounds tested, PPE-DABCO exhibited the highest virus inactivation activity, inducing more than 6 orders of magnitude of inactivation of both model viruses in the dark and with UV irradiation. The high antiviral activity of PPE-DABCO is likely due in part to its unique structural features. The polymer possesses the highest positive charge density on its side chains among the CPEs and OPEs tested in this study, which gives PPE-DABCO the ability to easily associate with the negatively charged viruses. In addition, the bulky side chains with highly hydrophobic yet positively charged groups of the PPE-DABCO prevent self-aggregation, thus making more of the polymer available to associate with the phage particles.

Our results also showed that all of the oligomers exhibit more efficient dark inactivation activity against the MS2 phage than the

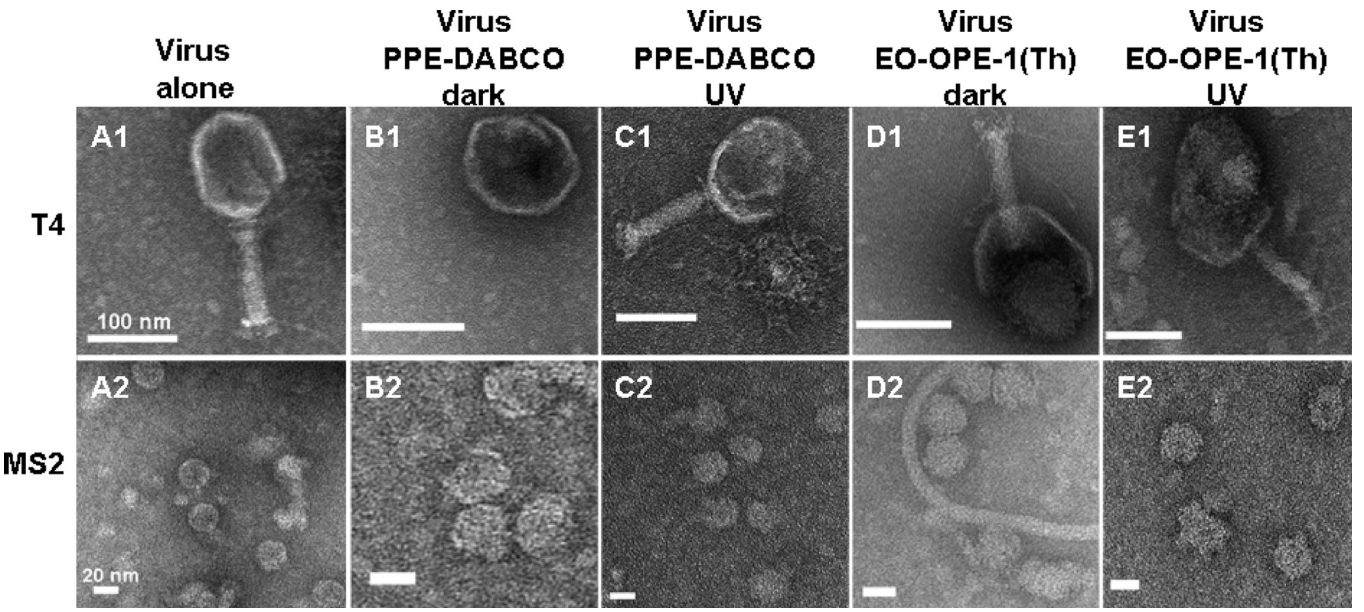

Figure 2. TEM images of the T4 and MS2 viruses alone (A1 and A2) and incubated with PPE-DABCO (B1 and B2, in the dark; C1 and C2, with UV irradiation) or EO-OPE-1 (Th) (D1 and D2, in the dark; E1 and E2, with UV irradiation) for one hour. The scale bars of the T4 images are 100 nm, and the scale bars of the MS2 images are 20 nm.

T4 phage. This could be due in part to the presence of 32 pores[14] (1.8 nm in diameter) on the MS2 capsid that provide easier access for the oligomers to interact with the packaged phage genome. It is also worth noting that long wavelength UV−visible light (LZC-420) alone produces negligible inactivation of the viruses (UV control data for polymeric PPE-DABCO and PPE-Th samples in Figure 1). In contrast, UVA irradiation in the absence of the oligomers causes measurable inactivation of both viruses (UV control data for oligomeric OPE-1, OPE-3, EO-OPE-1(C3), and EO-OPE-1(Th) samples in Figure 1). Moreover, UVA irradiation alone caused a higher level of virus inactivation of T4 compared to MS2. The different effects of UV light on the model viruses could be explained by T4's higher susceptibility to chemical damage. Upon exposure to UVA irradiation, adjacent thymidine residues in the by T4 phage DNA genome can covalently link to form thymidine dimers[16] and can to a lesser extent also induce protein−DNA photo-cross-linking leading the inactivation of T4 phage. While UVA can cause protein−RNA photo-cross-linking, RNA does not contain thymine, and uracil photodimerization is very rare.

It is clear from our data that the cationic CPE and OPE compounds tested show efficient inactivation activity against the two model viruses. The first step in viral infection is the recognition and binding of the viruses to the surface of the host cells. The T4 bacteriophage infection is initiated by the recognition of the lipopolysaccharides and the OmpC protein on the surface of host *E. coli* cells and followed by release of the phage genome into the host for replication.[17] Although the exact infection pathway of the MS2 phage is not clear, it is believed that the pilus of *E. coli* cells is a potential receptor for the MS2 phage.[18] The cationic CPEs and OPEs are expected to bind to the slightly negatively charged T4 and MS2 virus surfaces through electrostatic interactions. Thus, it is reasonable to assume that the antiviral activities of the CPE and OPE compounds are due in part from their ability to shield the virus particles from the host cells. Meanwhile, it is worth noting that because the sorption of the CPEs and OPEs to the viral particles is not fully understood, it is possible for the absorbed antiviral compounds to be desorbed with a change in the environmental conditions (such as solution pH and ionic strength) without causing lethal damage to the bacteriophages. We have shown previously that the CPE and OPE compounds can disrupt noncovalent biomolecular assemblies[11] and generate reactive oxygen species with UV−visible light exposure, which can strongly damage biomolecules, including proteins that make up the virus capsid.[10,19] We examined below if the binding of the compounds to virus particles results in further capsid damage.

PPE-DABCO and EO-OPE-1(Th) Disrupt Viral Morphology. To visualize the changes in viral morphology induced by PPE-DABCO and EO-OPE-1(Th), virus samples exposed to the compounds were imaged by TEM. Representative images (out of more than 10 collected) are shown in Figure 2. As a control, the untreated T4 phage shows its classic morphology with intact icosahedral head and tail structure (Figure 2A1).[17] In contrast, when exposed to PPE-DABCO or EO-OPE-1(Th), both in the dark as well as with UV light exposure, significant changes to the virus morphology are observed. As shown in Figure 2B1, the tail of the T4 phage is detached from the head in the presence of PPE-DABCO in the dark. Significant damage is also observed to the head of the T4 phage with the addition of PPE-DABCO in the light or with EO-OPE-1(Th) in the dark and under irradiation (Figure 2C1,D1,E1). Likewise, the untreated MS2 phage are uniformly sized and spherically shaped (Figure 2 A2). When exposed to PPE-DABCO and EO-OPE-1(Th) in the dark, the surface of the phage particles became rough and wrinkled (Figure 2B2,D2). MS2 phage treated with PPE-DABCO or EO-OPE-1(Th) with UV light irradiation exhibited significant disruption (Figure 2C2,E2).

EO-OPE-1(Th) Damages MS2 Capsid Protein with UV Irradiation. To assess the extent of damage to the virus capsid induced by the CPE and OPE compounds, the capsid proteins of the MS2 bacteriophage were analyzed with SDS-PAGE. The MS2 capsid is comprised of 180 copies of a coat protein with a

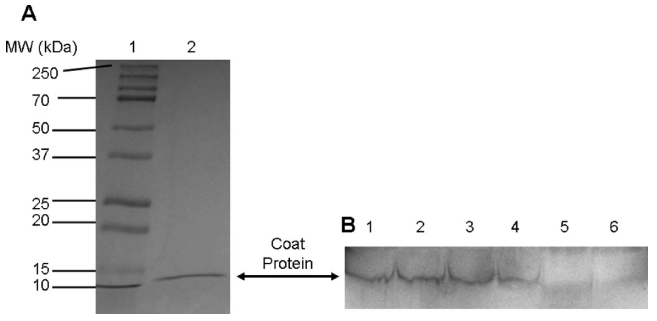

Figure 3. SDS-PAGE gels of the MS2 phage capsid. Lane A1, protein marker (BIO-RAD); lane A2 and B1, phage alone in the dark; lane B2, phage irradiated with UVA; lane B3, phage with 20 μg/mL EO-OPE-1(Th) in the dark; lane B4, phage with 40 μg/mL EO-OPE-1(Th) in the dark; lane B5, phage with 20 μg/mL EO-OPE-1(Th) irradiated with UVA; lane B6, phage with 40 μg/mL EO-OPE-1(Th) irradiated with UVA.

molecular weight of ~13.7 kDa and one copy of the maturase protein with a molecular weight of ~44 kDa.[6a,20] The band in lane 2 in Figure 3A from isolated MS2 phage particles is in agreement with expected molecular weight of the phage coat protein. Lanes 2−4 in Figure 3B show the coat protein band of viruses exposed to UVA irradiation alone and with EO-OPE-1(Th) in the dark. UV irradiation alone (Figure 3B, band 2) or the presence of EO-OPE-1(Th) in the dark (band 3 and 4) did not cause any significant changes to the coat protein band, indicating that these two conditions did not cause either aggregation or cleavage to the virus coat proteins. In contrast, the coat protein bands of MS2 in the presence of EO-OPE-1(Th) with UVA irradiation showed a band with significantly decreased intensity (Figure 3B, bands 5 and 6), indicating that the reactive oxygen species generated by the irradiation of EO-OPE-1(Th) has caused almost complete cleavage of the coat protein.[21] However, the degradation products have not been characterized in the present study.

MS2 phage inactivation data in Figure 1B show that the oligomer EO-OPE-1(Th) is very potent at inactivating the virus both in the dark and with UV irradiation, reducing the number of plaques by over 6 orders of magnitude. Our gel electrophoresis results show that virus inactivation in the dark and with UV irradiation proceeds through different mechanisms. No damage to the monomeric coat protein occurred with the virus particles exposed to the oligomer alone, implying that EO-OPE-1(Th) exerts its dark phage inactivation activity through physical binding to the phage particles, followed by possible remodeling of capsid architecture. Meanwhile, UV irradiation in the presence of the oligomer induced almost complete degradation of the virus coat protein. Thus, the mechanism of the antiviral properties of the CPEs and OPEs may be comprised of at least three parts: (1) Association of these cationic compounds with the virus particles attenuates virus recognition and binding to host cells. (2) The compounds disrupt the architecture or morphology of the virus capsid. (3) UV-induced generation of reactive oxygen species by the PPE-based compounds has the potential ability to covalently modify the capsid coat proteins.

SUMMARY AND CONCLUSIONS

In summary, the current study expands upon the utility of the PPE-based CPEs and OPEs as antimicrobials and it underscores that (1) most of these compounds exhibited high dark inactivation activity against the MS2 phage and moderate dark inactivation ability against the T4 phage through the inhibition of their infection pathway and/or the destruction of the virus structures, and (2) the UV light-enhanced antiviral activity of the CPEs and OPEs is achieved by the generation of corrosive reactive oxygen species, which can chemically damage the capsid protein of the model viruses. In ongoing studies, we are exploring in more detail the viral inactivation mechanism and efficacy of these materials in potential antiviral applications such as applying these materials as contact-active coatings using porous hydrogels and foams as substrates.

AUTHOR INFORMATION

Corresponding Author

*For E.Y.C.: phone, 1-505-277-2263; fax: 1-505-277-1979; E-mail, evachi@unm.edu. For D.G.W.: phone, 1-505-277-5736; fax, 1-505-277-1979; E-mail, Whitten@unm.edu.

ACKNOWLEDGMENT

This research is financially supported by the Defense Threat Reduction Agency (contract no. W911NF07-1-0079). We acknowledge Dr. Steven W. Graves at the Department of Chemical and Nuclear Engineering (UNM) for his help in phage growth, purification, and characterization. We thank Dr. David Peabody of Molecular Genetics & Microbiology (UNM) for his valuable instructions about bacteriophage. The TEM images were taken in the UNM Electron Microscopy Shared Facility, which is supported by the University of New Mexico Health Sciences Center and the University of New Mexico Cancer Center. We thank Dr. Stephen Jett for assistance with the TEM observation.

REFERENCES

(1) Weder, C. *Advances in Polymers Sciences*; Springer: New York, 2005; Vol. 177.

(2) (a) Bunz, U. H. F. *Chem. Rev.* **2000**, *100*, 1605–1644. (b) Thomas, S. W.; Joly, G. D.; Swager, T. M. *Chem. Rev.* **2007**, *107*, 1339–1386. (c) Hill, D. J.; Mio, M. J.; Prince, R. B.; Hughes, T. S.; Moore, J. S. *Chem. Rev.* **2001**, *101*, 3893–4011.

(3) (a) Chemburu, S.; Corbitt, T. S.; Ista, L. K.; Ji, E.; Fulghum, J.; Lopez, G. P.; Ogawa, K.; Schanze, K. S.; Whitten, D. G. *Langmuir* **2008**, *24*, 11053–11062. (b) Corbitt, T. S.; Ding, L. P.; Ji, E. Y.; Ista, L. K.; Ogawa, K.; Lopez, G. P.; Schanze, K. S.; Whitten, D. G. *Photochem. Photobiol. Sci.* **2009**, *8*, 998–1005. (c) Zhou, Z. J.; Corbitt, T. S.; Parthasarathy, A.; Tang, Y. L.; Ista, L. F.; Schanze, K. S.; Whitten, D. G. *J. Phys. Chem. Lett.* **2010**, *1*, 3207–3212.

(4) World Health Organization, *Global Summary of the AIDS Epidemic*, 2009.

(5) Moradpour, D.; Penin, F.; Rice, C. M. *Nature Rev. Microbiol.* **2007**, *5*, 453–463.

(6) (a) Kuzmanovic, D. A.; Elashvili, I.; Wick, C.; O'Connell, C.; Krueger, S. *Structure* **2003**, *11*, 1339–1348. (b) Rao, V. B.; Black, L. W. *Virol. J.* **2010**, *7*, 356–369. (c) Leiman, P. G.; Arisaka, F.; van Raaij, M. J.; Kostyuchenko, V. A.; Aksyuk, A. A.; Kanamaru, S.; Rossmann, M. G. *Virol. J.* **2010**, *7*, 355–382.

(7) Norder, H.; De Palma, A. M.; Selisko, B.; Costenaro, L.; Papageorgiou, N.; Arnan, C.; Coutard, B.; Lantez, V.; De Lamballerie, X.; Baronti, C.; Sola, M.; Tan, J.; Neyts, J.; Canard, B.; Coll, M.; Gorbalenya, A. E.; Hilgenfeld, R. *Antivir. Res.* **2011**, *89*, 204–218.

(8) Pasloske, B. L.; Walkerpeach, C. R.; Obermoeller, R. D.; Winkler, M.; DuBois, D. B. *J. Clin. Microbiol.* **1998**, *36*, 3590–3594.

(9) Brady-Estevez, A. S.; Schnoor, M. H.; Kang, S.; Elimelech, M. *Langmuir* **2010**, *26*, 19153–19158.

(10) Davies, M. J. *Biochem. Biophys. Res. Commun.* **2003**, *305*, 761–770.
(11) Wang, Y.; Tang, Y. L.; Zhou, Z. J.; Ji, E.; Lopez, G. P.; Chi, E. Y.; Schanze, K. S.; Whitten, D. G. *Langmuir* **2010**, *26*, 12509–12514.
(12) (a) Tang, Y. L.; Hill, E. H.; Zhou, Z. J.; Evans, D. G.; Schanze, K. S.; Whitten, D. G. *Langmuir* **2011**, *27*, 4945–4955. (b) Zhao, X. Y.; Pinto, M. R.; Hardison, L. M.; Mwaura, J.; Muller, J.; Jiang, H.; Witker, D.; Kleiman, V. D.; Reynolds, J. R.; Schanze, K. S. *Macromolecules* **2006**, *39*, 6355–6366.
(13) Hotze, E. M.; Badireddy, A. R.; Chellam, S.; Wiesner, M. R. *Environ. Sci. Technol.* **2009**, *43*, 6639–6645.
(14) Hooker, J. M.; Kovacs, E. W.; Francis, M. B. *J. Am. Chem. Soc.* **2004**, *126*, 3718–3719.
(15) Tang, Y. L.; Corbitt, S. C.; Parthasarathy, A; Zhou, Z. J.; Schanze, K. S.; Whitten, D. G. *Langmuir* **2011**, *27*, 4956–4962.
(16) Goodsell, D. S. *Oncologist* **2001**, *6*, 298–299.
(17) Furukawa, H.; Kuroiwa, T.; Mizushima, S. *J. Bacteriol.* **1983**, *154*, 938–945.
(18) Date, T. *Eur. J. Biochem.* **1979**, *96*, 167–175.
(19) Zheng, J.; Bizzozero, O. A. *Free Radical Res.* **2010**, *44*, 258–266.
(20) Peabody, D. S., *J. Nanobiotechnology* **2003**, *1*, doi: 10.1186/1477-3155-1-5.
(21) Neither cross-linked product nor cleaved product can be clearly visualized under current condition.